Article

Study on Top Hierarchy Control Strategy of AEBS over Regenerative Brake and Hydraulic Brake for Hub Motor Drive BEVs

Yu Yang *, Chao Wang, Shujun Yang and Xianzhi Tang

School of Vehicle and Energy, Yanshan University, No. 438 West Hebei Avenue, Qinhuangdao 066004, China
* Correspondence: nickyang@ysu.edu.cn

Abstract: A hub motor is an effective drive system for Battery Electric Vehicles (BEVs). However, due to limitations on packaging and cost, there are few applications in which hub motors are taken as the only actuators for a brake vehicle. Most applications involve a Regenerative Braking System (RBS) combined with a Hydraulic Braking System (HBS). In this paper, a top hierarchy Advanced Emergency Braking System (AEBS) controller is designed in Matlab/Simulink and State-flow, including functionalities of basic emergency braking, brake force distribution between front and rear wheels, anti-lock braking and coordination between RBS and HBS based on Model Predictive Control (MPC); a Seven Degrees of Freedom (DOF) BEV chassis model is constructed and rear-end crash test scenarios are created in Carsim with a high and low road adhesion coefficient. A series of comparison tests show that not only are the stopping distances between the ego vehicle and target vehicle shorter, but also the braking torques, longitudinal slip ratio and rotation speed of each wheel are well controlled without wheel locking. To sum up, in addition to meeting the AEBS requirements of avoiding a rear-end collision, the control strategy developed in this paper also levels up braking performance and enhances vehicle stability on both high-mu and low-mu roads for BEVs driven by a hub motor independently.

Keywords: battery electric vehicle; hub motor; advanced emergency braking system; regenerative braking; recuperative braking; hydraulic braking; distributed drive; model predictive control

1. Introduction

Hub motor technology is a hotspot of research to enhance vehicle stability via independent control of each wheel [1–3], from steering stability [4,5] to lateral handling [6,7]. Though some new solutions for hardware and software being developed to enhance vehicle braking performance [8–12], it is controversial whether Advanced Emergency Braking Systems (AEBS) can utilize a hub motor to enhance safety. Before proceeding to civilian motor vehicles, it is crucial to meet the brake requirements of an EV and comply with corresponding regulations and rules.

Because of this, most research on the combination of Regenerative Braking System (RBS) and Hydraulic Braking System (HBS) focuses on energy recovery and regenerative efficiency [13–16], and rarely on optimizing braking performance. Fuzzy logic control, sliding mode control and other control methods are also utilized to coordinate RBS and ABS [17–23], as are studies on Anti-lock Brake System (ABS) compatibility with RBS for an EV [24–27]. Model Predictive Control (MPC) is more popular to enhance course tracking and stability of motor vehicles [28–30]. Besides coordinating control between RBS and HBS, linear MPC is also used to optimize the motor torque [31], which gives us a new perspective to apply MPC in optimizing AEBS performance for a 4WD BEV.

This study's goal is to investigate a method of coordinating RBS and HBS to carry out the AEBS function for hub motor EVs. Along with creating a top hierarchy control strategy, an efficient logic for utilizing both RBS and HBS must be created. It is necessary to

improve braking performance rather than energy recovery by hub motors because AEBS are a higher-level system than other systems (e.g., Traction control), which is related to vehicle safety.

2. System Modelings

The content of this paper has certain novelties, and one of them is that a new architecture of RBS and HBS is designed for EVs driven by hub motors, including hardware for both RBS and HBS. In addition to hub motor inverters and battery pack, other sub systems are modeled based on the creative system layout below:

2.1. An Innovative Braking Architecture for BEV

Figure 1 shows two kinds of braking system are integrated in 4WD BEV architecture. One is HBS, based on the conventional hydraulic brake modulator; four control valves are added and regulated by the Hydraulic controller. The other is RBS, which utilizes hub motors to brake wheels. This is also called recuperative braking. Moreover, an AEBS controller is designed as the top hierarchy controller above the Hydraulic controller and Hub motor controller. According to signals from vehicle sensors (radar, wheel speed sensors, etc.), desired braking torque, wheel slip and state of the vehicle, etc., the AEBS controller calculates and determines required brake torque for HBS with RBS, to enhance the braking performance on different road conditions.
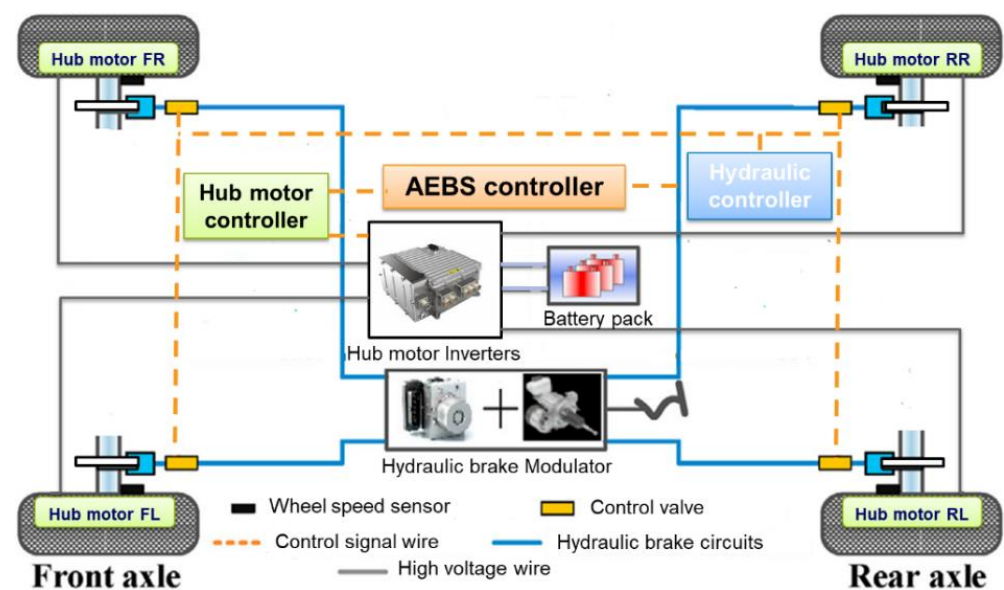

Figure 1. A novel braking architecture for 4WD BEV.

2.2. Vehicle Model

The 4WD BEV is modeled based on a Seven-Degree-Of-Freedom (7DOF) vehicle model, as demonstrated in Figure 2, and each DOF is defined in Table 1.

For this 4WD BEV dynamic model, Equations of longitudinal force, lateral force and Moment equation around z-axis are as follows:

$$m\left(\dot{V}_x - \gamma \cdot V_y\right) = \left(F_{x\_fl} + F_{x\_fr}\right)\cos\delta - \left(F_{y\_fl} + F_{y\_fr}\right)\sin\delta + F_{x\_rl} + F_{x\_rr}, \quad (1)$$

$$m\left(\dot{V}_y + \gamma \cdot V_x\right) = \left(F_{x\_fl} + F_{x\_fr}\right)\sin\delta + \left(F_{y\_fl} + F_{y\_fr}\right)\cos\delta + F_{y\_rl} + F_{y\_rr} \quad (2)$$

$$I_z \cdot \dot{\gamma} = \left[\left(F_{x\_fl} + F_{x\_fr} \right) \sin\delta + \left(F_{y\_fl} + F_{y\_fr} \right) \cos\delta \right] a + \left[\left(F_{x\_fr} - F_{x\_fl} \right) \cos\delta + \left(F_{y\_fl} - F_{y\_fr} \right) \sin\delta \right] \frac{t_{w1}}{2} + \left(F_{x\_rr} - F_{x\_rl} \right) \frac{t_{w2}}{2} - \left(F_{y\_rl} + F_{y\_rr} \right) b, \tag{3}$$

$$\begin{cases} F_{z\_fl} = mg\frac{b}{2l} - m\dot{V}_x \frac{h_g}{2l} - m\dot{V}_y \frac{h_g}{t_{w1}} \cdot \frac{b}{l} \\ F_{z\_fr} = mg\frac{b}{2l} - m\dot{V}_x \frac{h_g}{2l} + m\dot{V}_y \frac{h_g}{t_{w1}} \cdot \frac{b}{l} \\ F_{z\_rl} = mg\frac{a}{2l} + m\dot{V}_x \frac{h_g}{2l} - m\dot{V}_y \frac{h_g}{t_{w2}} \cdot \frac{a}{l} \\ F_{z\_rr} = mg\frac{a}{2l} + m\dot{V}_x \frac{h_g}{2l} + m\dot{V}_y \frac{h_g}{t_{w2}} \cdot \frac{a}{l} \end{cases} \tag{4}$$
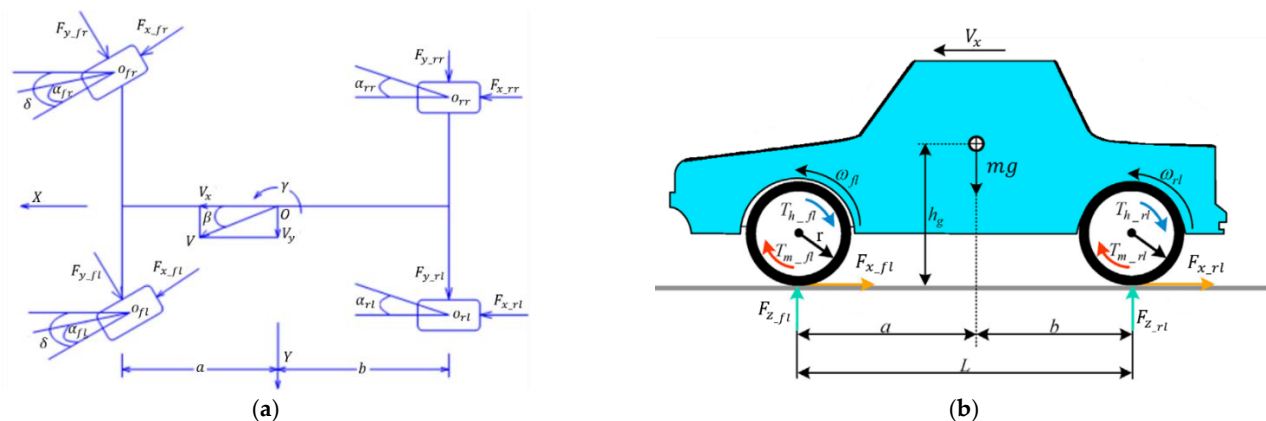
where m is the sprung mass of the BEV; V_x, V_y are the longitudinal speed and lateral speed of the BEV; γ is yaw rate of the BEV; F_{x_fl}, F_{x_fr}, F_{x_rl}, F_{x_rr} are the longitudinal force on each wheel from the ground, respectively (e.g.,: F_{x_fl}, represents force on Left Front wheel); F_{y_fl}, F_{y_fr}, F_{y_rl}, F_{y_rr} are the lateral force on each wheel from the ground separately; δ is the steering wheel angle (only front wheels are steering wheels in this model); I_z is the yaw inertia, which is the BEV inertia around Z-axis; a, b are the longitudinal distance from mass center of gravity to the centerline of the front axle and the rear axle, respectively; t_{w1}, t_{w2} are the track width of front and rear wheels; F_{Z_fl}, F_{Z_fr}, F_{Z_rl}, F_{Z_rr} are the vertical force on each wheel from the ground, respectively; h_g is the vertical distance between the mass center of gravity and the ground; and l is the wheelbase of the BEV. a, b, l follow the equation below:

$$l = a + b \tag{5}$$

Since the brake force is supplied by two system, RBS and HBS, the equation of forces on each wheel is expressed as the following:

$$\begin{cases} J\dot{\omega}_{fl} = F_{x\_fl}r - T_{m\_fl} - T_{h\_fl} \\ J\dot{\omega}_{fr} = F_{x\_fr}r - T_{m\_fr} - T_{h\_fr} \\ J\dot{\omega}_{rl} = F_{x\_rl}r - T_{m\_rl} - T_{h\_rl} \\ J\dot{\omega}_{rr} = F_{x\_rr}r - T_{m\_rr} - T_{h\_rr} \end{cases}, \tag{6}$$

where J is the moment of inertia of the wheel; $\omega_{fl}, \omega_{fr}, \omega_{rl}, \omega_{rr}$ are the rotation speeds of each wheel; r is the rolling radius of the wheel (here, it is assumed the moment of inertia and radius of each wheel are the same); $T_{m\_fl}, T_{m\_fr}, T_{m\_rl}, T_{m\_rr}$ are the RBS torque generated by hub motor for each wheels, respectively; $T_{h\_fl}, T_{h\_fr}, T_{h\_rl}, T_{h\_rr}$ are the HBS torque on each wheels, separately.

Figure 2. 7DOF 4WD BEV dynamic model: (**a**) Longitudinal and lateral force on 7DOF model; (**b**) The force and torques on left wheels.

Table 1. DOF Definitions of 7DOF vehicle model.

Movements	Directions	DOF
Rotational movement of four wheels	Around wheel centerline	4
Longitudinal movement of vehicle	Along X-axis	1
Lateral movement of vehicle	Along Y-axis	1
Yaw of vehicle	Around Z-axis	1

2.3. Tire Model

The tire model of this 4WD BEV is based on Pacejka's renowned MF-Tire mode, which is an implementation of the world-standard Pacejka Magic Formula tire model [32,33]. It can be described as follows:

$$
\begin{cases}
F_{xji} = Dsin(Ctan^{-1}\{B\lambda_{ij} - E[B\lambda_{ij} - tan^{-1}(B\lambda_{ij})]\}); \\
C = a_0; \\
D = \mu(a_1 F_{zij}^2 + a_2 F_{zij}); \\
B = a_3 sin(a_4 \arctan(a_5 F_{zij}))/CD; \\
E = a_6 F_{zij}^2 + a_7 F_{zij} + a_8;
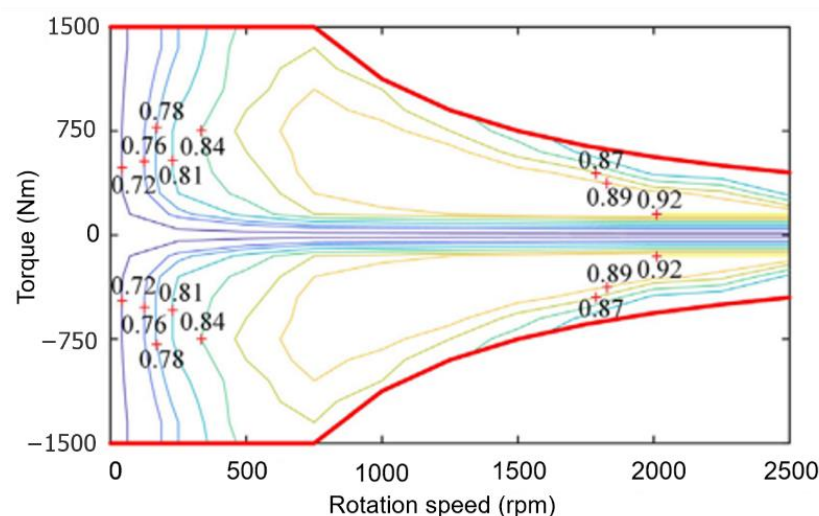\end{cases}
\tag{7}
$$

where F_{xij} is the longitudinal force on each tire (e.g.,: F_{xfl} represents longitudinal force on left front tire); μ is the adhesion coefficient between road and tire; B is the tire stiffness coefficient; C is the tire shape factor; D is the crest factor of the tire; E is the tire curvature factor; and $a_0, a_1, a_2, a_3 \cdots a_8$ are MF-tire model parameters according to experiments results; F_{zij} is the vertical force on tires; λ_{ij} is the longitudinal slip ratio of each wheel, and it can be calculated with the following equations:

$$
\lambda_{ij} = \frac{r\omega_{ij} - V_{t\_ij}}{V_{t\_ij}},
\tag{8}
$$

where V_{t_ij} are the longitudinal velocities of center point of each tire, separately, per tire coordination system.

2.4. RBS Model

Four identical hub motors are used in this 4WD BEV architecture, whose model is created according to the map illustrated in Figure 3.

Figure 3. The efficiency map of hub motor.

The relationship between power, rotation speed and efficiency of the hub motor can be written as the following equation:

$$P_m = \begin{cases} \frac{T_m n_m}{9550 \eta_m} & driving \\ \frac{T_m n_m \eta_m}{9550} & braking \end{cases} \tag{9}$$

where P_m is the power of the hub motor; T_m is the output torque of the hub motor; n_m is the rotation speed of the hub motor, which is equal to wheel rotation speed; η_m is the hub motor efficiency.

2.5. HBS Model

The hydraulic pressure in each wheel cylinder is controlled independently by HBS [34]. Here, it is assumed that the braking torque generated by the mechanism of brake disc and pad, and hydraulic pressure regulated by each control valve, is actuating on the wheel cylinder to push the brake pad. To sum up, the relation between braking torque generated by HBS and pressure in each wheel cylinder is defined as follows:

$$\begin{cases} T_{h\_fl} = \frac{1}{4(\tau s + 1)} \pi r d_{fl}^2 \psi_{b\_fl} P_{W\_fl}; \\ T_{h\_fr} = \frac{1}{4(\tau s + 1)} \pi r d_{fr}^2 \psi_{b\_fr} P_{W\_fr}; \\ T_{h\_rl} = \frac{1}{4(\tau s + 1)} \pi r d_{rl}^2 \psi_{b\_rl} P_{W\_rl}; \\ T_{h\_rr} = \frac{1}{4(\tau s + 1)} \pi r d_{rr}^2 \psi_{b\_rr} P_{W\_rr}; \end{cases} \tag{10}$$

where P_{W_fl}, P_{W_fr}, P_{W_rl}, and P_{W_rr} are pressure measured in each wheel cylinder, separately; d_{fl}. d_{fr}, d_{rl}, and d_{rr} are piston diameters of each wheel cylinder, respectively; ψ_{b_fl}, ψ_{b_fr}, ψ_{b_rl}, and ψ_{b_rr} are the braking efficiency factors of the each wheel; τ is the time constant related to the structure of the HBS.

2.6. Battery Model

Since we take vehicle safety as the top priority when developing the AEBS control strategy, energy recovery efficiency of RBS is less emphasized. Here, a simplified battery model is adopted as the following equation [35]:

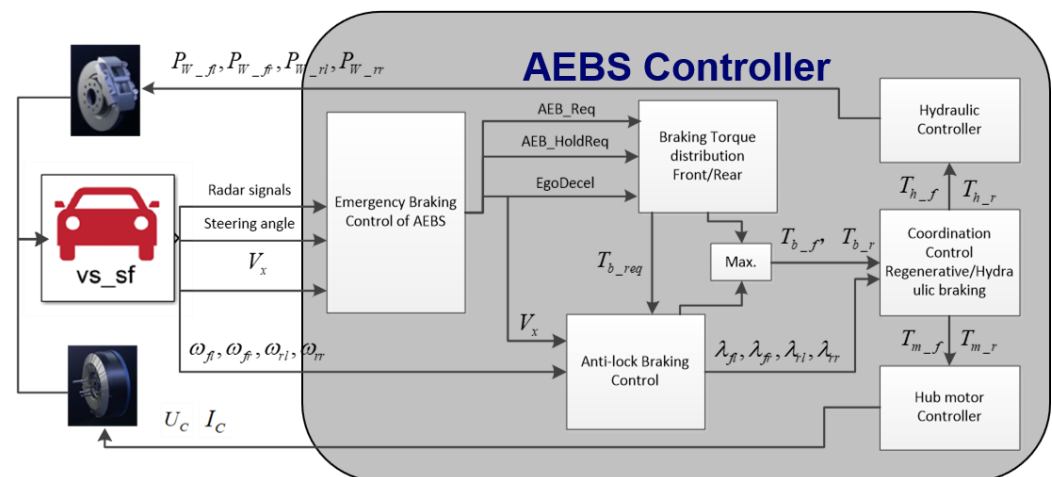$$\eta = \frac{U_C I_C}{\sum\limits_{i=1, j=1}^{2} \omega_{m\_ij} T_{m\_ij}} \tag{11}$$

the η is the charging efficiency from hub motors to the battery when RBS; U_C represents the battery charging voltage when RBS; I_C is the current generated by RBS; T_{m_ij} is RBS torque generated by each hub motor (e.g.,: T_{m_12} is the brake torque from the front right hub motor); ω_{m_ij} is the rotation speed (angular velocity) for each hub motor, respectively;

Additionally, the charging power of the battery P_C can be described in the following equation:

$$P_C = U_C I_C \tag{12}$$

3. AEBS Control Strategy

In this study, the AEBS control module is developed in Matlab/Simulink, whose architecture is demonstrated in Figure 4:

Figure 4. Architecture of the AEBS controller.

The AEBS controller not only calculates the status of a vehicle using signals from radar or other sensors to detect a potential collision, requesting torque on time to avoid rear-end collision or reduce crash severity, but also distributes braking torque between front and rear wheels between RBS and HBS. It makes full use of the road adhesion by requesting torque on demand to make wheels anti-lock in order to handle tough road conditions, such as snow, mud, and ice, and to enhance the braking performance of this 4WD BEV.

Several key control logics are integrated in the AEBS controller, and details on each control strategy are specified as follows:

3.1. AEBS Basic Functionalities

3.1.1. Functionalities Definitions

AEBS control logic is to perform two basic functionalities: collision warning (FCW) and emergency braking. Here, since how to coordinate RBS and HBS to level up emergency braking performance regardless road adhesion condition is crucial to collision avoidance or damage mitigation, the control strategy of emergency braking will be further analyzed rather than FCW in the paper. Usually, validation on control strategy of AEBS functions is divided into three categories [36], as shown below:

- CCRs: Car-to-Car Rear Stationary;
- CCRm: Car-to-Car Rear Moving;
- CCRb: Car-to-Car Rear Braking.

Because of the sufficient complexities and high representative, a test scenario of CCRb is focused on and the corresponding control logic is further investigated below.

3.1.2. Generic Control Logic

TTC (Time-To-Collision) is used as a key control parameter. It is the value of time obtained by dividing the longitudinal distance (in the direction of travel of the subject vehicle) between the subject (ego) and the target vehicle by the longitudinal relative speed of the ego and target vehicle. It is also vital to determine the degree of emergency and imminence of collision to trigger the braking request to the preceding control module; for instance, braking torque distribution between front and rear wheels [37].

As shown in Figure 5, the AEBS basic control strategy is based on the assumption that the ego vehicle and target vehicle both run at a certain acceleration, and only when the velocity of the ego vehicle is higher than the velocity of the target vehicle is AEBS function triggered and TTC calculated in the specific control module.
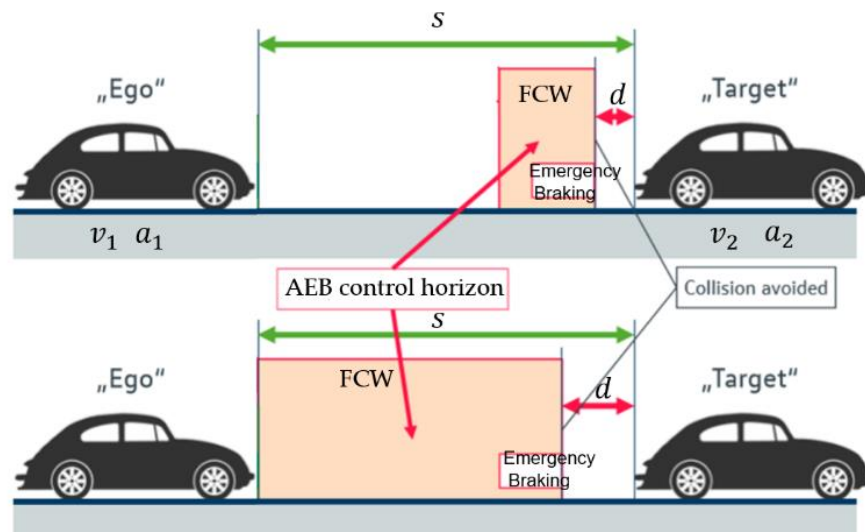
Figure 5. Schemes for AEBS control logic in CCRb.

First, assuming the ego vehicle and the target vehicle run at certain speed, and at a certain time, brake at certain deceleration, eventually, the velocity of both will reach zero, which is expressed as the following equation:

$$v_2t + \frac{1}{2}a_2t^2 + (s-d) = v_1t + \frac{1}{2}a_1t^2 \tag{13}$$

where v_1, v_2 is the velocity of the ego vehicle and the target vehicle, respectively; a_1, a_2 is the acceleration (or deceleration) of the ego vehicle and the target vehicle, separately; s is the distance between the ego vehicle and the target vehicle when both start braking; d is the safety distance between the ego vehicle and the target vehicle which is set in the AEBS controller according to OEM's specifications (0.5–3 m is recommended);

v_{rel}, a_{rel} are defined as the relative speed and relative acceleration between the ego vehicle and the target vehicle, respectively, and they meet the following equation:

$$\begin{cases} v_{rel} = v_1 - v_2 \\ a_{rel} = a_1 - a_2 \end{cases} \tag{14}$$

Based on Equations (15) and (16), TTC can be calculated with the following equation:

$$TTC = \begin{cases} t = \frac{s-d}{v_{rel}} & (a_{rel} = 0) \\ t = \frac{-v_{rel}+\sqrt{v_{rel}^2+2a_{rel}(s-d)}}{a_{rel}} & (a_{rel} \neq 0) \end{cases} \tag{15}$$

3.1.3. CCRb Control Logic

In scenario CCRb, the control strategy is more complex than that for CCRs and CCRm. Moreover, some prerequisites are essential to detect the situation and make decisions; for example, whether the target vehicle stops earlier than the ego vehicle or any collision happens before the target vehicle stop.

Supposing ego vehicle and target vehicle decelerate at a_1, a_2, respectively, from different vehicle speed v_1, v_2; finally, both stop at the same time. Then, we have the following equation:

$$a_1v_2 = a_2v_1 \tag{16}$$

However, this is quite ideal; most situations are divided into two possibilities:

1.   The ego vehicle decelerates faster than the target vehicle and stops before the target vehicle stops, which is $|a_1v_2| \leq |v_1a_2|$. The minimum distance between the two

vehicles is when the velocities of both vehicles are the same, and the TTC for this test scenario is calculated the same as in Equation (17);

2. The ego vehicle decelerates slower than the target vehicle, which is $|a_1 v_2| > |v_1 a_2|$; then, the shortest distance between the two vehicles could happen before the target vehicle stops, or after it stops. If $v_1 \left| \frac{v_2}{a_2} \right| + \frac{1}{2} a_1 \left| \frac{v_2}{a_2} \right|^2 < \left| \frac{v_2^2}{2a_2} \right| + s - d$, then there is no collision before target vehicle stop and the minimum distance between the two vehicle is after the target vehicle stop. Based on Equation (17), the TTC for this scenario is calculated as shown below:

$$TTC = \begin{cases} t = \dfrac{s - d + \left| \frac{v_2^2}{2a_2} \right|}{v_1} & (a_1 = 0) \\ t = \dfrac{-v_1 + \sqrt{v_1^2 + 2a_1 \left(s - d + \left| \frac{v_2^2}{2a_2} \right| \right)}}{a_1} & (a_1 \neq 0) \end{cases} \quad (17)$$

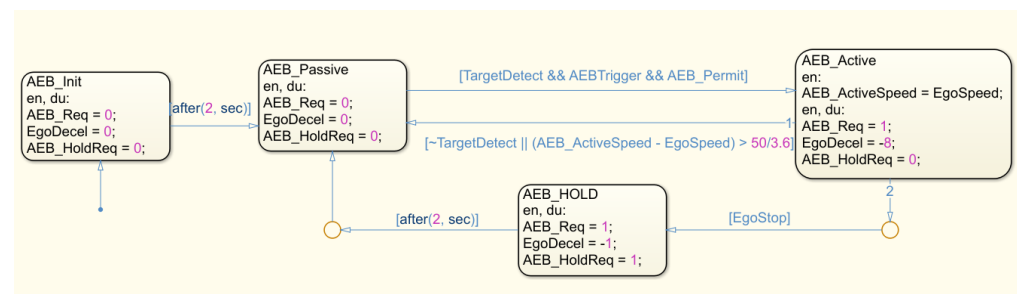3. If $v_1 \left| \frac{v_2}{a_2} \right| + \frac{1}{2} a_1 \left| \frac{v_2}{a_2} \right|^2 \geq \left| \frac{v_2^2}{2a_2} \right| + s - d$, then there may be a chance of collision before the target vehicle stops, and the minimum distance between the two vehicles is also before the target vehicle stops. Derived from Equation (17), the TTC for this scenario is calculated as the following equation:

$$TTC = \begin{cases} t = \dfrac{s - d}{v_{rel}} & (a_{rel} = 0) \\ t = \dfrac{-v_{rel} + \sqrt{v_{rel}^2 + 2a_{rel}(s - d)}}{a_{rel}} & (a_{rel} \neq 0) \end{cases} \quad (18)$$

3.1.4. Control Module Design in Matlab/Stateflow

Based on the analysis and calculations above, the basic AEBS functionalities of emergency braking are designed and modeled in Matlab/Stateflow as shown below.

In Figure 6, four states are designed in Stateflow: AEBS initiate (AEB_Init), System Passive (AEB_Passive), System active (AEB_Active) and Brake Holding (AEB_Hold). Moreover, inputs for state switch are signals from Radar sensor (Target Detect), a combination signal from BMS (including seat belt, doors), ESP, steering angle and TTC (calculated from ego vehicle and target vehicle); additionally, there is a lower speed threshold for system function, and here, it is set to 50 km/h. Outputs are AEB request signal (AEB_Req), brake deceleration request (EgoDecel) and brake holding request (AEB_HoldReq), which can make the vehicle hold still for 2 s after the vehicle completely stops, to avoid any slippage in case of steep slopes or hills.
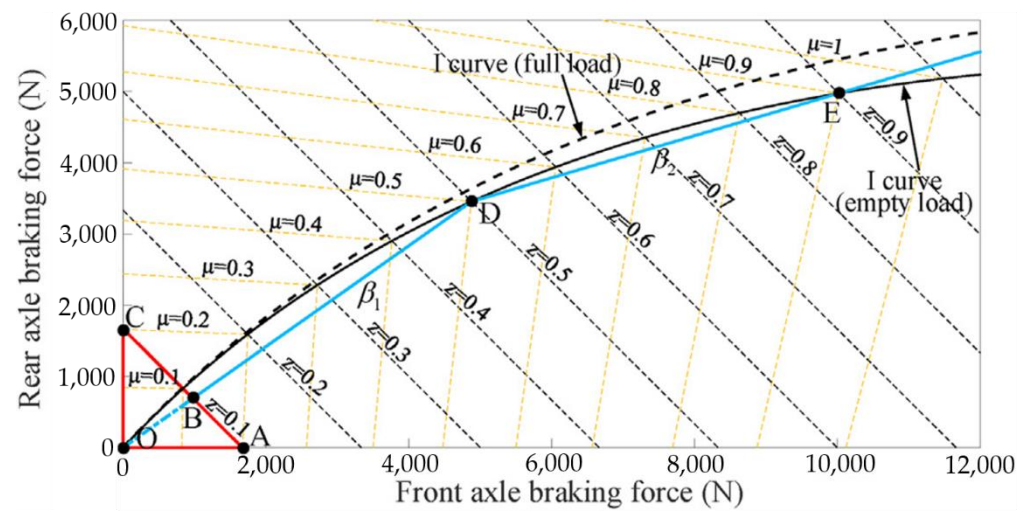

Figure 6. Control logic of AEBS basic functions in Stateflow.

3.2. Torque Distribution between Front and Rear Wheels

The control strategy for braking force distribution between the front and rear axles is designed according to the regulation ECE R13, as illustrated in Figure 7, as follows:

Figure 7. Control map for braking force distribution between the front and rear axles.

When $z \leq 0.1$, there are no specific restrictions according to the ECE regulation. Since the braking force of the front and rear axles is relatively small, HBS alone can cover braking requirements by providing sufficient braking force. On the contrary, the hub motor is running at low efficiency when torque output is relatively low. Therefore, braking force distribution between the front and rear axles by RBS and HBS is designed as follows:

$$\begin{cases} T_{m\_f} = 0 \\ T_{m\_r} = 0 \\ T_{h\_f} = \beta_1 T_{b\_req} \\ T_{h\_r} = (1 - \beta_1) T_{b\_req} \end{cases} \tag{19}$$

where T_{m_f}, T_{h_f} are the braking torques output by RBS and HBS on the front axle, respectively; T_{m_r}, T_{h_r} are the braking torques on rear axle by RBS and HBS, separately; T_{b_req} is the total amount of braking toque requested by AEBS per current vehicle state against target vehicle and road condition.

For $0.1 < z \leq 0.5$, the braking force distribution between the front and rear axles is following β_1 line. Because of the fast response of output torque from hub motor, RBS is prioritized to meet the requirements on braking strength. If this is not sufficient, the remaining part of the total braking torque requirement is provided by the HBS according to the following equation:

$$\begin{cases} T_{m\_f} = \min(\beta_1 T_{b\_req}, \frac{2T_{m\_max}(n)}{\eta}) \\ T_{m\_r} = \min((1 - \beta_1) T_{b\_req}, \frac{2T_{m\_max}(n)}{\eta}) \\ T_{h\_f} = \beta_1 T_{b\_req} - T_{m\_f} \\ T_{h\_r} = (1 - \beta_1) T_{b\_req} - T_{m\_r} \end{cases} \tag{20}$$

where $T_{m\_max}(n)$ is the maximum torque that the hub motor can provide at speed n; η is the mechanical efficiency from hub motor to wheels.

When $z > 0.5$, the proportion between front braking torque and rear braking torque is set based on the look-up table of the β_2 line. Four hub motors are also prioritized to meet

the requirements of total braking torque and braking strength. The rest of the required braking torque is provided by the HBS as well, as calculated below:

$$
\begin{cases}
T_{m\_f} = \min(\beta_2 T_{b\_req}, \frac{2T_{m\_\max}(n)}{\eta}) \\
T_{m\_r} = \min((1 - \beta_2) T_{b\_req}, \frac{2T_{m\_\max}(n)}{\eta}) \\
T_{h\_f} = \beta_2 T_{b\_req} - T_{m\_f} \\
T_{h\_r} = (1 - \beta_2) T_{b\_req} - T_{m\_r}
\end{cases}
\tag{21}
$$

To sum up, the core of this control module on braking torque distribution between the front and rear axle is to utilize hub motor torque at maximum. Higher torque and quick torque response is a great advantage of RBS, which is essential for boosting the braking performance and vehicle safety.

3.3. Anti-Lock Control Module Design

To utilize the maximum lateral force and longitudinal force of tire, longitudinal adherence coefficient should be kept near the peak value and set between 8% and 30% [38]. Longitudinal slip ratios of each wheel are calculated according to Equation (8). Logic threshold control method is adopted with two acceleration thresholds, one deceleration threshold and two thresholds of longitudinal wheel slip ratio, whose model is designed in Matlab/Stateflow.

3.4. Coordinationg Control Strategy for RBS and HBS

3.4.1. State Estimator Model

The Model Predictive Control method is used to coordinate the RBS and HBS torque, and the 3DOF vehicle dynamics model is chosen as an estimator of the vehicle state, including the longitudinal movement of the vehicle, the rotational movement of the front and rear wheels, and the state and control variables, which are defined as following equation:

$$
X = \begin{bmatrix} x_1 \\ x_2 \end{bmatrix} = \begin{bmatrix} \omega_{mf} \\ \omega_{mr} \end{bmatrix}
\tag{22}
$$

$$
U = \begin{bmatrix} u_1 \\ u_2 \end{bmatrix} = \begin{bmatrix} T_m \\ T_h \end{bmatrix}
\tag{23}
$$

where ω_{mf}, ω_{mr} are the rotation speeds of the front and rear hub motors, respectively (assuming the left and right wheel in the same axle rotate at the same speed, since there is no steering); T_m is the total amount of torque for RBS; T_h is the total amount of torque for HBS; T_m, T_h are both defined as positive.

Then, based on Equations (4) and (6), the state equations can be described as follows:

$$
\begin{aligned}
\dot{x}_1 &= \frac{1}{2J} \left[\mu_f F_{zf} r - (u_1 + u_2) \frac{k}{1+k} \right] \\
\dot{x}_2 &= \frac{1}{2J} \left[\mu_r F_{zr} r - (u_1 + u_2) \frac{k}{1+k} \right]
\end{aligned}
\tag{24}
$$

where μ_f, μ_r are the longitudinal slip ratio of the front and rear wheels, separately; F_{zf}, F_{zr} are the vertical force on the front axle and rear axle, respectively; k is the ratio of front axle braking torque to rear axle braking torque.

3.4.2. Cost Function

To provide enough braking torque to each wheel and boost the braking stability, two cost functions are designed here to optimize the required braking torque distribution

between the front and rear axle, and their unified objective is to be the minimum in the current predictive horizon, as shown below:

$$
\begin{aligned}
J_1(k) &= J_1(u(k|k), u(k+1|k), \dots u(k+N_p-1|k)) \\
&= P_1 \sum_{i=1}^{N_p} \|s_1(k+i|k) - s_r\|^2 + Q_1 \sum_{i=1}^{N_p-1} \|\Delta T_b(k+i|k)\|^2
\end{aligned}
\tag{25}
$$

$$
\begin{aligned}
J_2(k) &= J_2(u(k|k), u(k+1|k), \dots u(k+N_p-1|k)) \\
&= P_2 \sum_{i=1}^{N_p} \|s_2(k+i|k) - s_r\|^2 + Q_2 \sum_{i=1}^{N_p-1} \|\Delta T_{b\_req}(k+i|k)\|^2
\end{aligned}
\tag{26}
$$

where $k+1|k$ represents the prediction of parameter states at time $k+1$ based on the states at time k; s_r is the target value of longitudinal slip ratio for each wheel; P_1 and P_2 are the weight coefficients for enhancing the braking safety; Q_1 and Q_2 are weight coefficients that guarantee that the torque capacity of both braking systems will meet vehicle requirements for different road conditions. T_b is the sum of braking torque provided by RBS and HBS together, which is $T_b = T_m + T_h$.

3.4.3. Constrains

Due to the fast response of hub motor torque, the cost functions are mainly constrained by the braking torque received by the wheels, the changing rate of braking torque and the longitudinal slip ratio range for each wheel, defined as the following equations:

$$
\begin{cases}
T_{b\_f}{}^{min} \le T_{b\_f}(k+i|k) \le T_{b\_f}{}^{max} \\
T_{b\_r}{}^{min} \le T_{b\_r}(k+i|k) \le T_{b\_r}{}^{max}
\end{cases}
\tag{27}
$$

$$
\begin{cases}
\Delta T_h{}^{min} \le \Delta T_{h\_ij}(k+i|k) \le \Delta T_h{}^{max} \\
\Delta T_m{}^{min} \le \Delta T_{m\_ij}(k+i|k) \le \Delta T_m{}^{max}
\end{cases}
\tag{28}
$$

$$
\begin{cases}
s_f{}^{min} \le s_f(k+i|k) \le s_f{}^{max} \\
s_r{}^{min} \le s_r(k+i|k) \le s_r{}^{max}
\end{cases}
\tag{29}
$$

where $T_{b\_f}{}^{min}$ and $T_{b\_r}{}^{min}$ are the minimum braking torques requested by AEBS controller to the front and rear wheels, respectively; $T_{b\_f}{}^{max}$ and $T_{b\_r}{}^{max}$ are the maximum value of braking torques requested by AEBS for the front and rear wheels, separately; $\Delta T_h{}^{min}$ and $\Delta T_h{}^{max}$ are the lower and upper limitation of the torque changing rate for HBS; $\Delta T_m{}^{min}$ and $\Delta T_m{}^{max}$ the lower limitation and upper limitation of torque changing rate for RBS s; $s_f{}^{min}$ and $s_r{}^{min}$ are the minimum value of longitudinal slip rate of front wheels and rear wheels, respectively; $s_f{}^{max}$ and $s_r{}^{max}$ are the maximum value of the longitudinal slip rate of front and rear wheels, separately.

3.4.4. Control Module Design

According to Equations (25) and (26), two weight coefficients are proposed, plus three cost functions related to total braking torque. The rate of torque change and the longitudinal slip ratio range are derived from Equations (27)–(29). Moreover, the estimator model is described in state-space format as Equations (22) and (23), and MPC performance is evaluated with the plant model and modeled based on Matlab MPC toolbox.
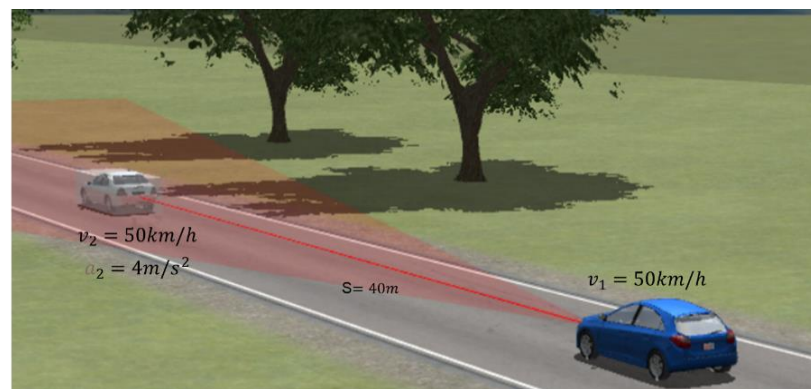
4. Simulation and Analysis

To verify the AEBS control strategy, including control logic for automatic emergency braking, we use a control strategy for braking torque distribution between front and rear axle, anti-lock braking control logic and coordination between RBS and HBS based on MPC. A 4WD BEV model is established based on the Matlab/Simulink platform, whose key parameters are shown in Table 2.

Table 2. Key parameters of the 4WD BEV.

Definition	Symbols	Value
Sprung mass of vehicle	m	1270 kg
Longitudinal distance from mass center of gravity to centerline of front axle	a	1015 mm
Longitudinal distance from mass center of gravity to centerline of rear axle	b	1895 mm
Height of sprung mass center of gravity	h_g	540 mm
Rolling radius of tire	r	325 mm
Total Moment inertia of wheel, tire and hub motor	J	4.5 kg·m^2
Yaw inertia of vehicle	I_z	1540 kg·m^2

According to GB/T 39901-2021, a representative tricky test scenario is chosen (the ego vehicle is running at 50 km/h, 40 m away from the target vehicle, which brakes with 4 m/s^2 deceleration) to verify the control strategy, as illustrated in Figure 8. Test scenarios are built in Carsim and several comparison tests are designed between RBS + HBS and HBS only. Furthermore, simulations on emergency braking performance are carried out on roads with both a high adhesion coefficient and a low adhesion coefficient with the platform of Matlab/Simulink co-simulation with Carsim.

Figure 8. AEBS test scenario in Carsim.

4.1. Braking Performance

To validate the AEBS control strategy, four simulation tests are designed to compare the braking performance by RBS + HBS and by HBS only, as well as the distance between the ego vehicle and the target vehicle when both the stop and time to stop for the ego vehicle are measured in the simulation platform on roads with a high and low adhesion coefficient. The test results are shown in Table 3.

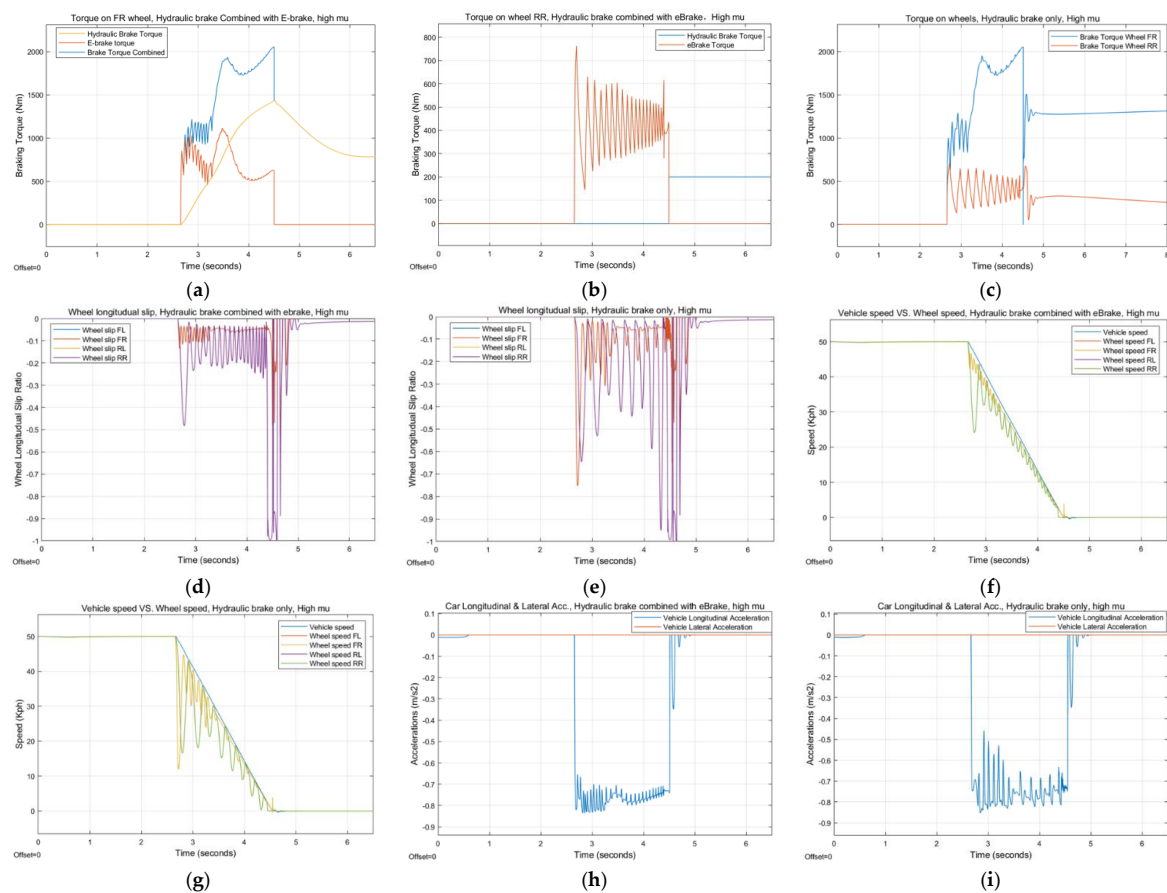**Table 3.** AEBS simulation tests results.

Mechanism of Braking	Road Condition	Distance between Ego Vehicle and Target Vehicle When Both Stop	Time to Stop
RBS + hydraulic	$\mu = 0.85$	1.49 m	4.5 s
Hydraulic only	$\mu = 0.85$	1.34 m	4.6 s
RBS + hydraulic	$\mu = 0.3$	1.36 m	6.3 s
Hydraulic only	$\mu = 0.3$	0.82 m	7.6 s

The target distance between the ego vehicle and the target vehicle when both stop is set as 1.5 m, and road condition does have some impact on braking distance either caused

by road condition or the response time of the braking mechanism. However, the control strategy completes the emergency braking function by coordinating RBS and HBS as a top hierarchy controller. Additionally, braking distance and time to brake are both better improved by RBS + HBS than that by HBS only; in particular, the braking distances are so well controlled that they are nearly equal to our target value (1.5 m).

4.2. Braking Stability

Since the road conditions for both the left and right wheel are the same, neither steering scenario nor yaw control is considered in this paper. Wheel FR and wheel RR are taken as examples to illustrate the force (torque), longitudinal slip and rotation speed for wheels on the front and rear axle, respectively. As shown in Figure 9a,b, as soon as RBS and HBS receive torque requests from AEBS controller, its anti-lock braking function activates immediately and regulates the braking torque on both the front and rear wheels. Due to relatively low torque requirements for rear wheels, rear wheels are braked by RBS alone. Once the ego vehicle stops, RBS reduces torque to zero immediately, but HBS maintains pressure for at least 2 s in case of the car sliding on steep slope. On the contrary, braking torques on both front and rear wheels which are regulated by HBS only have more severe and intense fluctuation than that by RBS + HBS, as compared with Figure 9c.

Figure 9. Simulation results for AEBS validation in high μ road. (μ = 0.85) (**a**) Total braking torque, torque of RBS and HBS on wheel FR of ego vehicle; (**b**) torque of RBS and HBS on wheel RR of ego vehicle; (**c**) HBS torque on wheel FR and wheel RR of ego vehicle; (**d**) longitudinal slip ratio of wheels of ego vehicle, RBS + HBS; (**e**) longitudinal slip ratio of wheels of ego vehicle, HBS only; (**f**) vehicle speed vs. wheel speed of ego vehicle, RBS + HBS; (**g**) vehicle speed vs. wheel speed of ego vehicle, HBS only; (**h**) longitudinal and lateral acceleration of ego vehicle, RBS + HBS; (**i**) longitudinal and lateral acceleration of ego vehicle, HBS only.

In addition, as shown in Figure 9d,e, with coordination control of RBS and HBS, the longitudinal slip ratios of both front and rear wheels for an ego vehicle are less fluctuated and more convergent towards to the target slip ratio than those modulated by HBS only.

By comparing Figure 9f,g, another finding is that none of the ego vehicle wheels are locked, proving that the functions of the anti-lock control strategy are well designed. However, wheel speeds of the ego vehicle controlled by RBS +HBS are changing less and approaching the vehicle speed faster than those modulated by HBS only. In addition to coordinating RBS and HBS, this shows the AEBS control strategy terrifically enhances braking performance, which is why braking distance is also decreased.

Last but not least, as can be seen by comparing Figure 9h with Figure 9i, both RBS and HBS are significantly well coordinated to achieve higher deceleration and full utilization of road adhesion. Furthermore, difference on lateral acceleration between RBS +HBS and HBS only is not that obvious as a result of the same road conditions for both the left and right wheel. However, thanks to coordination control logic between RBS and HBS, longitudinal accelerations of ego vehicle fluctuate less than a vehicle braked by HBS only, which also strengthen the braking stability of BEV.

Another set of contrast simulation results is shown in the following figures.

Similar to the previous analysis, comparing Figure 10a,b with Figure 10c, we show that braking torque coordinated by AEBS controller over RBS and HBS has a faster and more accurate response than that with HBS only. RBS alone can meet the torque requirement of rear wheels due to the relatively low braking torque required on a low μ road, Additionally, the function of automatic holding is available; the torque of HBS remains as soon as the ego vehicle stops and the RBS torque is back to zero.
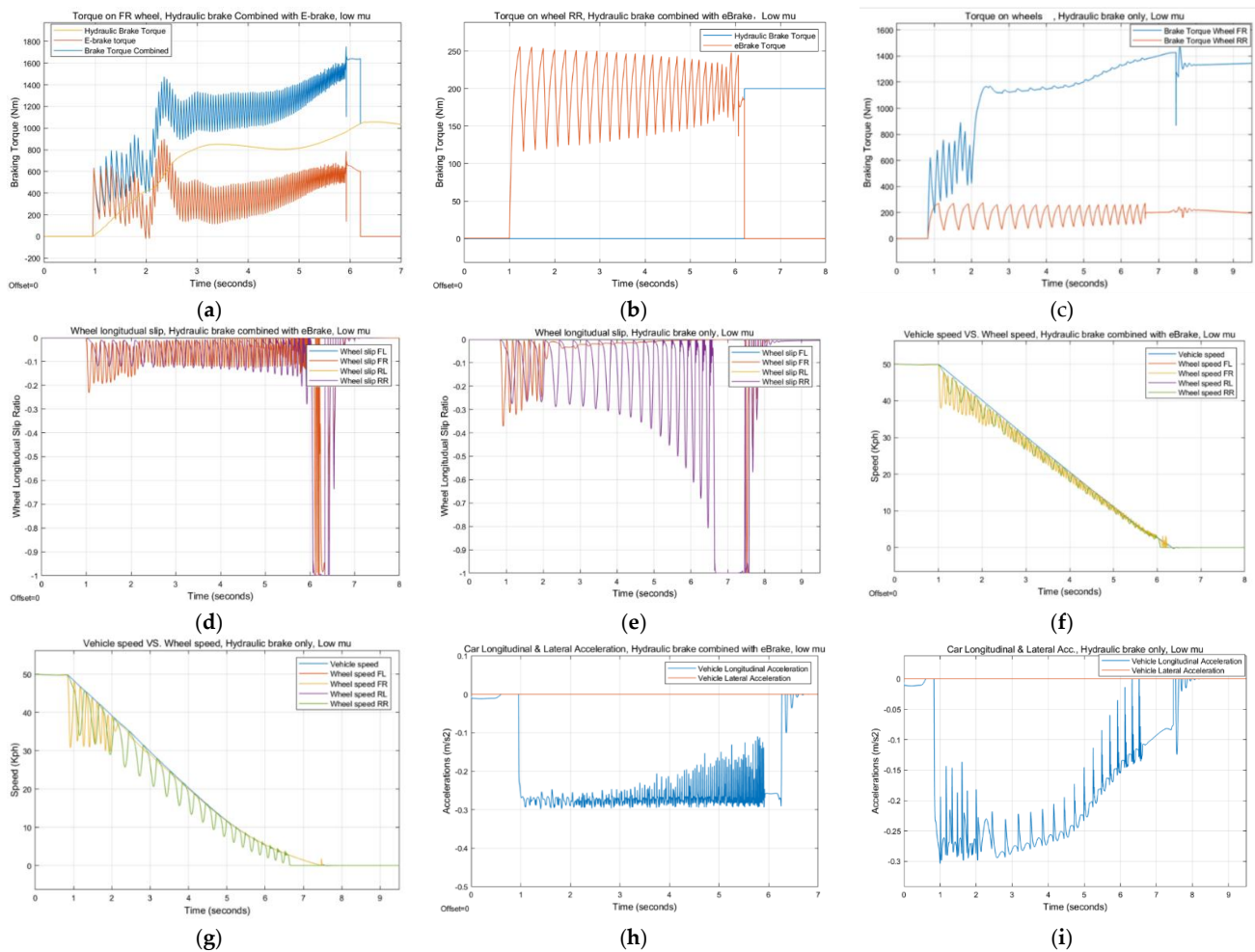
Moreover, comparisons between Figure 10d,e demonstrate that without coordination control of RBS and HBS, longitudinal slip ratios of both front and rear wheels tend to fluctuate more severely and intensely. However, due to white noise from sensors on simulations models in Carsim, there are still some strong signals of longitudinal slip ratios after the ego vehicle stop, which can be ignored in this analysis.

By comparing Figure 10f with Figure 10g, one finding is that with the help of coordination control between RBS and HBS, the time taken to brake is shorter and the braking distance is greatly reduced; thanks to the anti-lock control strategy integrated in AEBS controller, none of the wheels on the ego vehicle are locked.

Last but not least, as can be seen from Figure 10h–i, coordination control logic between RBS and HBS works better than that controlled by HBS alone in both longitudinal and lateral accelerations, which significantly result in higher deceleration and full utilization of road adhesion of the ego-vehicle.

To sum up, other novelties of this study are: by utilizing quick response and high accuracy of hub motor torque, anti-lock brake frequency is raised as the stopping distance is shortened, which verifies that AEBS performance is enhanced on both high μ and low μ road. Furthermore, both energy recuperative efficiency and vehicle active safety are taken into consideration, as the cost function and constraints of the Model Predictive Control algorithm to coordinate RBS and HBS to optimize AEBS, achieving higher deceleration and full utilization of road adhesion.

Figure 10. Simulation results for AEBS control strategy validation in low μ road. (μ = 0.3) (**a**) Total braking torque, torque from RBS and HBS on wheel FR of ego vehicle; (**b**) RBS and HBS torque on wheel RR of ego vehicle; (**c**) HBS torque on wheel FR and wheel RR of ego vehicle; (**d**) longitudinal slip ratio of ego vehicle wheels, RBS + HBS; (**e**) longitudinal slip ratio of ego vehicle wheels, HBS only; (**f**) ego vehicle speed vs. wheel speed, RBS + HBS; (**g**) ego vehicle speed vs. wheel speed, HBS only; (**h**) longitudinal and lateral acceleration of ego vehicle, RBS + HBS; (**i**) longitudinal and lateral acceleration of ego vehicle, HBS only.

5. Conclusions

This aspect of the research suggested that the hub motor can enhance the braking performance of a 4WD BEV on some tough road conditions by designing a top hierarchy control strategy of AEBS, whose function of avoiding rear-end collision is well verified on both high-mu and low-mu roads. Furthermore, these findings provide a potential mechanism for a perfect balance of energy recuperative efficiency and vehicle active safety. Thanks to coordination of RBS and HBS and optimization of brake torque by an MPC algorithm, the longitudinal slip ratios of each wheel are well controlled and road adhesion is fully utilized to achieve higher brake performance, proving that the AEBS control strategy integrated with brake force distribution, anti-lock braking and coordination of RBS and HBS is successfully developed and verified.

1. In future work, validations of the AEBS on other test scenarios might prove important, including scenario of CCRs (Car-to-Car Rear Stationary) and CCRm (Car-to-Car Rear Moving), or more harsh road conditions; for example, the split μ road and step μ road.

References

1. Kerem, B. Performance comparison of electric-vehicle drivetrain architectures from a vehicle dynamics perspective. *Proc. Inst. Mech. Eng. Part D-J. Automob. Eng.* **2020**, *234*, 915–935.
2. Xin, C.; Yang, W.M.; Yao, Y.F. Electric car design based on wheel motor drive. In Proceedings of the 7th International Forum on Industrial Design, Yongzhou, China, 17–19 May 2019.
3. Li, J. Research Status and Development Prospect of Electric Vehicles Based on Hub Motor. In Proceedings of the China International Conference on Electricity Distribution (CICED), Tianjin Univ, Tianjin, China, 17–19 September 2018; pp. 126–129.
4. Guo, X.R.; Yi, C.; Chen, L.H.; Li, H. Research on Steering Stability Control of Electric Vehicle Driven by Dual In-Wheel Motor. In Proceedings of the 10th Institute-of-Electrical-and-Electronics-Engineers International Conference on Cyber Technology in Automation, Control, and Intelligent Systems (CYBER), Xian, China, 10–13 October 2020; pp. 394–399.
5. Hou, R.F.; Li, Z.; Sun, T.M. Steering Stability Control for a Four Hub-Motor Independent-Drive Electric Vehicle with Varying Adhesion Coefficient. *Energies* **2018**, *11*, 2438. [CrossRef]
6. Li, S.T.; Liu, H.; Zhao, D.; Li, Q.Y.; Tian, Y.T.; Wang, D.J.; Yu, D.L. Adaptive Sliding Mode Control of Lateral Stability of Four Wheel Hub Electric Vehicles. *Int. J. Automot. Technol.* **2020**, *21*, 739–747. [CrossRef]
7. Zhang, H.Z.; Liang, J.S.; Jiang, H.B.; Cai, Y.F.; Xu, X. Stability Research of Distributed Drive Electric Vehicle by Adaptive Direct Yaw Moment Control. *IEEE Access* **2019**, *7*, 106225–106237. [CrossRef]
8. Sergey, P.; Kasper, R. Development and Validation of a New Kind of Coupling Element for Wheel-Hub Motors. In Proceedings of the International Scientific Conference on Mechanics—Eighth Polyakhov's Reading, Saint Petersburg, Russia, 20–24 June 2018.
9. Anupam, K.; Vishwakarma, K.; Maram, D.; Malik, A. In-wheel Motor for Solar Electric Vehicles: Challenges and Opportunities. In Proceedings of the 1st International Conference on Advances in Mechanical Engineering and Nanotechnology (ICAMEN), Jaipur, India, 8–9 March 2019.
10. Tan, N.; Yan, H.S. On the Design of In-Wheel-Hub Motor Transmission Systems with Six-Link Mechanisms for Electric Vehicles. *Energies* **2018**, *11*, 2920.
11. Sun, X.D.; Zhou, S.; Cai, Y.F.; Lei, G.; Guo, Y.G.; Zhu, J.G. Driving-Cycle-Oriented Design Optimization of a Permanent Magnet Hub Motor Drive System for a Four-Wheel-Drive Electric Vehicle. *IEEE Trans. Transp. Electrif.* **2020**, *6*, 1115–1125. [CrossRef]
12. Fan, Y.; Gu, C.L. Power Supply System Design and Dynamic Analysis of a Permanent Magnet Bistable Electromagnetic Clutch for Wheel Motor Drive. *IEEE Access* **2020**, *8*, 218161–218169.
13. Li, G.; Yang, Z. Energy saving control based on motor efficiency map for electric vehicles with four-wheel independently driven in-wheel motors. *Adv. Mech. Eng.* **2018**, *10*, 1–18.
14. Zhang, L.W.; He, R. Research on multi-mode RBS energy recovery of electric vehicle with double rotor hub motor. *Int. J. Veh. Des.* **2020**, *82*, 45–63. [CrossRef]
15. Wang, Y.J.; Xie, M.W.; Yi, D.H. Research and Verification of Cooperative RBS Function Based on Electrical Brake Booster System. In Proceedings of the China SAE Congress, Shanghai, China, 27–29 October 2018; pp. 933–948.
16. Li, Y.; Adeleke, O.P.; Xu, X. Methods and applications of energy saving control of in-wheel motor drive system in electric vehicles: A comprehensive review. *J. Renew. Sustain. Energy* **2019**, *11*, 1–22. [CrossRef]
17. He, L.; Ye, W.; He, Z.; Song, K.; Shi, Q. A combining sliding mode control approach for electric motor anti-lock braking system of battery electric vehicle. *Control. Eng. Pract.* **2020**, *104*, 104520. [CrossRef]
18. De Castro, R.; Araujo, R.E.; Freitas, D. Wheel slip control of EVs based on sliding mode technique with conditional integrators. *IEEE Trans. Ind. Electron.* **2013**, *60*, 3256–3271. [CrossRef]
19. Basrah, M.S.; Siampis, E.; Velenis, E.; Cao, D.; Longo, S. Wheel slip control with torque blending using linear and nonlinear model predictive control. *Veh. Syst. Dyn.* **2017**, *55*, 1665–1685. [CrossRef]
20. Shi, J.; Wu, J.; Zhu, B.; Zhao, Y.; Deng, W.; Chen, X. Design of anti-lock braking system based on RBS for distributed drive electric vehicle. *Int. J. Passeng. Cars-Electron. Electr. Syst.* **2018**, *11*, 205–218. [CrossRef]
21. Qiu, C.; Wang, G.; Meng, M.; Shen, Y. A novel control strategy of RBS for electric vehicles under safety critical driving situations. *Energy* **2018**, *149*, 329–340. [CrossRef]
22. Aksjonov, A.; Vodovozov, V.; Augsburg, K.; Petlenkov, E. Design of regenerative anti-lock braking system controller for 4 in-wheel-motor drive electric vehicle with road surface estimation. *Int. J. Automot. Technol.* **2018**, *19*, 727–742. [CrossRef]
23. Zhang, J.; Yang, Y.; Qin, D.; Fu, C.; Cong, Z. RBS Control Method Based on Predictive Optimization for Four-Wheel Drive Pure Electric Vehicle. *IEEE Access* **2021**, *9*, 1394–1406. [CrossRef]
24. Song, D.F.; Yang, D.P.; Zeng, X.H.; Zhang, X.M.; Gao, F.W. A coordinated control of hydraulic hub-motor auxiliary system for heavy truck. *Measurement* **2021**, *175*, 109087. [CrossRef]

25. Yu, D.; Wang, W.; Zhang, H.; Xu, D. Research on anti-lock braking control strategy of distributed-driven electric vehicle. *IEEE Access* **2020**, *8*, 162467–162478. [CrossRef]
26. Pretagostini, F.; Ferranti, L.; Berardo, G.; Ivanov, V.; Shyrokau, B. Survey on wheel slip control design strategies, evaluation and application to antilock braking systems. *IEEE Access* **2020**, *8*, 10951–10970. [CrossRef]
27. Li, S.S.; Guo, L.P.; Zhang, B.C.; Lu, X.H.; Cui, G.J.; Dou, J.L. MPC-based Slip Control System for In-wheel-motor Drive EV. In Proceedings of the 5th International-Federation-of-Automatic-Control (IFAC) Conference on Engine and Powertrain Control, Simulation and Modeling (E-COSM), Changchun, China, 20–22 September 2018; pp. 578–582.
28. Li, Z.; Wang, C.P.; Hou, Y.H.; Liu, C. MPC-Based Integrated Control of Trajectory Tracking and Handling Stability for Intelligent Driving Vehicle Driven by Four Hub Motor. *IEEE Trans. Veh. Technol.* **2022**, *71*, 2668–2680.
29. Li, S.; Li, Z.; Zhang, B.; Zheng, S.; Lu, X.; Yu, Z. *Path Tracking for Autonomous Vehicles Based on Nonlinear Model: Predictive Control Method*; SAE Technical Paper 2019-01-1017; SAE: Detroit, MI, USA, 2019.
30. Zeng, X.H.; Li, G.H.; Yin, G.D.; Song, D.F.; Li, S.; Yang, N.N. Model predictive control-based dynamic coordinate strategy for hydraulic hub-motor auxiliary system of a heavy commercial vehicle. *Mech. Syst. Signal Process.* **2018**, *101*, 97–120. [CrossRef]
31. Yu, Z. *Automobile Theory*, 6th ed.; China Machinery Industry Press: Beijing, China, 2018.
32. Pacejka, H.B. *Tire and Vehicle Dynamics*, 3rd ed.; Butterworth-Heinemann: Oxford, UK, 2012.
33. Pacejka, H.B.; Besselink, I.J.M. Magic Formula Tire model with Transient Properties. *Suppl. Veh. Syst. Dyn.* **1997**, *27*, 234–249. [CrossRef]
34. Zhao, X.Y.; Xu, W.B.; Liu, G. Pressure Estimation and Pressure Control of Hydraulic Control Unit in Electric-Wheel Vehicle. *Math. Probl. Eng.* **2020**, *2020*, 6576297. [CrossRef]
35. Yang, Z.; Wang, B.; Jiao, K. Life cycle assessment of fuel cell, electric and internal combustion engine vehicles under different fuel scenarios and driving mileages in China. *Energy* **2020**, *198*, 117365. [CrossRef]
36. Hu, N.X.; Wang, J.; Wu, K. Test and Research of Commercial Vehicle Advanced Emergency Braking Pedestrian System. In Proceedings of the China SAE Congress, Shanghai, China, 27–29 October 2022; Springer: Singapore, 2022; Volume 769.
37. Guo, J. Development of RBS for electric vehicles in China: A review. *Int. J. Electr. Hybrid Veh. IJEHV* **2015**, *7*, 120–138. [CrossRef]
38. Xu, W.; Zhao, H.; Ren, B.; Chen, H. A RBS control strategy for electric vehicle with four in-wheel motors. In Proceedings of the 2016 35th Chinese Control Conference (CCC), Chengdu, China, 27–29 July 2016; pp. 8671–8676.